Genetic modification of *Clostridium kluyveri* for heterologous *n*-butanol and *n*-hexanol production

Caroline Schlaiß[a,b], Saskia T. Baur[b], James W. Marsh[c], Kurt Gemeinhardt[b], Largus T. Angenent[a,b,d,e,f,,#]

[a]AG Angenent, Max Planck Institute for Biology, Max-Planck-Ring 5, 72076Tübingen, Germany

[b]Environmental Biotechnology Group, Department of Geosciences, University of Tübingen, Schnarrenbergstraße 94-96, 72076 Tübingen, Germany

[c]Department of Microbiome Science, Max Planck Institute for Biology, Max-Planck-Ring 5, 72076 Tübingen, Germany

[d]The Novo Nordisk Foundation CO_2 Research Center (CORC), Aarhus University, Gustav Wieds Vej 10C, 8000 Aarhus C, Denmark

[e]Department of Biological and Chemical Engineering, Aarhus University, Gustav Wieds Vej 10D, 8000 Aarhus C, Denmark

[f]Cluster of Excellence – Controlling Microbes to Fight Infections, University of Tübingen, Auf der Morgenstelle 28, 72074 Tübingen, Germany

Running Head: Heterologous *n*-butanol and *n*-hexanol production of *C. kluyveri*

#Address correspondence to Largus T. Angenent, l.angenent@uni-tuebingen.de

*Present address: Largus T. Angenent, Department of Geosciences, University of Tübingen, Schnarrenbergstraße 94-96, 72076 Tübingen, Germany

Abstract: 218 words

ABSTRACT

The mesophilic microbe *Clostridium kluyveri* serves as the most commonly used model microbe to elucidate the physiology and biochemistry of ethanol-based chain elongation *via* reverse ß-oxidation. In this pathway, ethanol and acetate are converted into short- and medium-chain carboxylates. However, to date, no genetic system has been published in a peer-reviewed publication. Here, we report the development of versatile genetic tools for *C. kluyveri*, utilizing the pMTL *Clostridia* shuttle vector system and thiamphenicol as a selective marker. We identified the native restriction-modification system of *C. kluyveri* as a critical barrier to DNA transfer and overcame it by identifying and characterizing the crucial methyltransferase. To mimic the native DNA methylation pattern of *C. kluyveri*, we performed *in-vivo* methylation of the shuttle vector plasmid by expressing the methyltransferase in *Escherichia coli*, followed by DNA transfer *via* conjugation. After validating the genetic system, we demonstrated heterologous expression of different combinations of both NADH and NADPH-dependent alcohol dehydrogenases from *Clostridium acetobutylicum*. The expression of these genes was controlled by the P_{thl} promoter, which is commonly used in *Clostridia,* and the P_{adhE2} promoter, leading to *n*-butanol and *n*-hexanol production of the mutant strains. This genetic system for *C. kluyveri* will not only enable further research on the metabolism of this microbe but also enable more profound insights into ethanol-based chain elongation in general.

IMPORTANCE

Medium-chain carboxylates are required in various everyday products, including cosmetics, pharmaceuticals, and fragrances, and show a natural antimicrobial property. Further, they represent food additives and serve as chemical building blocks for several other compounds. Traditionally, these carboxylates are produced from fossil resources, contributing to increased greenhouse gas emissions. Alternatively, they are derived from animal- or plant-based fat (*e.g.*, coconut oil), which competes with agricultural land that is needed for food production. However, microbial chain elongation, which is a biotechnological approach relying on microbes, such as *Clostridium kluyveri*, is sustainable and a promising alternative to the conventional production of medium-chain carboxylates. Notably, it enables the use of industrial waste streams (*e.g.*, off-gases, carbohydrate-rich industrial waste) as substrates, making the process more environmentally friendly. By applying our genetic system for *C. kluyveri*, a better understanding of microbial chain elongation can be achieved, and potentially even an extension of its product portfolio.

INTRODUCTION

Despite advances in renewable energy technologies, modern society remains heavily dependent on fossil fuels. This continued reliance contributes considerably to greenhouse gas emissions, which in turn accelerate climate change and the depletion of natural resources (1). Therefore, moving toward a more circular economy represents a critical challenge for sustainability to ensure long-term resilience for future generations. A key aspect of this transformation is the development of sustainable alternatives for essential chemical building blocks, which are conventionally assembled using fossil resources.

The development of sustainable alternatives represents a central challenge for modern environmental biotechnology. In particular, chemical building blocks that are in high demand from industry include short- and medium-chain carboxylates (SCCs and MCCs, respectively) (2). Both SCCs and MCCs contain a carboxylic group; while SCCs have carbon chains with a length of two to five carbon atoms, MCCs consist of six to twelve carbons (3) and their monetary value increases with an increasing chain length (4). MCCs serve as versatile chemical compounds with numerous industrial applications. Beyond functioning as essential building blocks for bioplastics (5, 6) and potential biofuel precursors through Kolbe electrolysis (7-9), these compounds have considerable utility across multiple sectors. They are widely incorporated into cosmetics, pharmaceuticals (2), fragrances (10), and rubber production (11). Additionally, MCCs feature prominently in food products as flavor additives (11, 12) and in animal feed formulations, where they provide valuable antimicrobial properties (13, 14). Also, they serve as precursors for alcohols such as *n*-butanol and *n*-hexanol (15). Conventionally, MCCs are produced from petrochemicals (16), leading to environmental devastation and mobilization and release of carbon dioxide (CO_2). A

potential bio-alternative that is already applied on an industrial scale is the production of MCCs from animal or plant fat, for example, coconut oil, palm kernel oil, and castor oil (17, 18). However, the sustainability of this approach is contested because it requires agricultural land, which is indispensable for growing food, especially given the steadily increasing global population (19). Another promising biotechnological alternative is microbial chain elongation to produce MCCs.

By using the reverse ß-oxidation pathway, microbes fuse a C2 compound to short-chain carboxylates, resulting in a stepwise elongation of the carbon chain by two carbon atoms at a time, respectively, up to a maximum chain length of six carbon atoms (20). This elongation process can be achieved by reactor microbiomes using an open culture of microbial consortia. The open cultures do not require sterile treatment and are resilient to disturbances (21, 22). Another promising attempt, which was demonstrated in several studies, is to couple syngas fermentation with chain elongation by cultivating an acetogenic and a chain-elongating microbe in a co-culture (23-26). First, the acetogenic microbe produces the intermediates ethanol and acetate from a mixture of hydrogen, CO_2, and carbon monoxide. Second, the chain-elongating microbe further elongates the intermediates to medium-chain carboxylates *via* reverse ß-oxidation. Third, the acetogenic microbe reduces SCCs and MCCs into their corresponding alcohol (*n*-butanol and *n*-hexanol). Besides open- and co-cultures, medium-chain carboxylate production performed by pure cultures offers higher production rates (27).

Clostridium kluyveri has been extensively used to study the physiology and biochemistry of ethanol-based chain elongation *via* the reverse ß-oxidation pathway (28-31). Therefore, it serves as a model microbe for microbial chain elongation. To date, no genetic system for this microbe has been published in a peer-reviewed study. Here, we developed a genetic system for *C. kluyveri* by mimicking its native

methylation pattern on a shuttle vector plasmid to circumvent its restriction-modification defense system. As a proof of principle, we introduced and heterologously expressed alcohol dehydrogenases from *Clostridium acetobutylicum* to enable *n*-butanol and *n*-hexanol production. By applying the findings from this study, metabolic engineering of *C. kluyveri* can be used to increase its productivity, expand its product portfolio, and obtain more profound insights into the reverse ß-oxidation metabolism in general.

118 # RESULTS

119 ## Plating optimization

120 To enable successful genetic modification, our initial focus was to optimize plating
121 conditions for the reliable growth of single colonies, because a high plating efficiency
122 increases the likelihood of isolating the correct clone. We systematically adjusted each
123 variable to determine the optimal plating conditions. Of these, supplementing the
124 DSMZ52 medium with a 10-fold concentration of vitamins and using cells in their early
125 exponential growth phase had the most substantial positive impact on colony formation
126 (**Table S1**). Other modifications, such as pour-plating with 0.8% Bacto agar, increasing
127 the atmospheric pressure in the storage tanks to 0.6 bar, and placing a sterile filter
128 paper (1 cm × 1 cm) soaked with ethanol in the lid of the Petri dish to ensure sufficient
129 substrate supply, showed moderate positive effects (**Table S1**).
130 In contrast, using complex modified Reinforced Clostridial Medium (RCM) (32), which
131 was supplemented with 20 mL/L ethanol and 2.5 g/L $NaHCO_3$ instead of DSMZ52
132 medium, and adding ethanol to the external plate atmosphere affected the plating
133 efficiency negatively (**Table S1**). Further, using paper clips to increase ventilation
134 resulted in a drastic reduction in colony formation (**Table S1**), most likely due to ethanol
135 evaporation and plate desiccation from the enhanced airflow. Because hydrogen
136 production of *C. kluyveri* resulted in large bubbles of the pour-plated medium, which
137 complicated post-treatment, we decided to perform spread-plating whenever a minor
138 reduction in plating efficiency was acceptable. For routine plating, we chose DSMZ52
139 medium with increased vitamin supplementation over RCM to reduce contamination
140 risk and improve consistency. However, RCM medium was necessary during
141 conjugation to support the growth of *E. coli*.
142

143 **Antibiotic testing**

144 Selection of cells carrying the desired plasmid requires two key factors: **1)** the
145 sensitivity of the wild-type strain to the respective antibiotic, and **2)** the expression of
146 an enzyme that ensures resistance to the antibiotic to which the wild-type strain is
147 sensitive. Thiamphenicol resistance is a well-established marker in many clostridial
148 strains, including strains closely related to *C. kluyveri* (33, 34). Therefore, we tested
149 the sensitivity of the cells to thiamphenicol in liquid DSMZ52 medium and on plates
150 and determined the minimum inhibitory concentration (MIC) after one week, which was
151 3 µg/mL (**Figure S1**). However, we chose to use a higher concentration of 5 µg/mL
152 thiamphenicol in liquid medium to prevent the growth of wild-type cells due to
153 spontaneous resistance or a reduction in antibiotic concentration caused by instability
154 of the antibiotic at 37°C after prolonged incubation. Additionally, we used this
155 concentration to select plasmid-carrying cells on solid media.

156

157 **Identification of the crucial methylation pattern**

158 A restriction assay of the pMTL83151 shuttle vector plasmid (35), using the cell lysate
159 of *C. kluyveri*, showed digestion of the foreign DNA, producing fragment sizes of
160 approximately 2 kbp and 0.5 kbp (**Figure 1A**). This result indicated that the native
161 restriction and modification defense system of *C. kluyveri* (**Figure 1B**) is a critical
162 barrier that must be overcome for successful genetic modification. PacBio sequencing
163 of the native methylation pattern of the genomic DNA of *C. kluyveri* DSM555 revealed
164 methylation at the following DNA sites: GATC, GWTAAT, CCAAG, CAAAAAT, and
165 CCGG, suggesting the presence of multiple restriction-modification systems. *In-silico*
166 analysis revealed that the observed restriction pattern of the unmethylated pMTL83151
167 corresponded to the CCGG as the critical methylation site, corresponding with the
168 findings of Schneider, 2024 (36).

169 We identified a native methyltransferase in the REBASE database (37) that methylates
170 CCGG sites and is encoded by the genome of *C. kluyveri* (locus tag CKL_2671). To
171 counteract the restriction, we expressed this methyltransferase under the control of the
172 Isopropyl-ß-D-thiogalactopyranoside (IPTG)-inducible P_{lac} promoter on the plasmid
173 pMeth (**Figure 2**) to mimic *C. kluyveri*-specific methylation of pMTL83151. As a result,
174 the restriction assay testing CCGG-methylated pMTL83151 showed reduced plasmid
175 digestion. Next, we optimized the methyltransferase expression by testing different
176 IPTG concentrations (10-1000 mM) for induction in *E. coli* TOP10. In a final restriction
177 digest (**Figure 1C**), we only observed minimal digestion of the shuttle vector after 24 h,
178 indicating that the restriction sites of the foreign DNA were protected by methylation
179 (**Figure 1D**). The lowest restriction activity occurred at IPTG induction concentrations
180 between 200 mM and 500 mM right after inoculation. Based on these results, we
181 established 500 mM IPTG as the standard concentration for inducing the expression
182 of the methyltransferase.
183

184 **Triparental conjugational DNA transfer**

185 The *E. coli* TOP10 strain, harboring both pMTL83151 and pMeth plasmids, exhibited
186 reduced growth rates. This growth inhibition was likely attributable to the metabolic
187 burden that was imposed by maintaining resistance to two antibiotics simultaneously
188 (chloramphenicol for pMTL83151 and ampicillin for pMeth), combined with the
189 additional cellular stress of protein expression that is induced by IPTG treatment. To
190 avoid additional burden on this strain by introducing a third plasmid to enable
191 conjugation, we instead performed triparental mating for shuttle vector transfer into the
192 *C. kluyveri* recipient using a modified transformation protocol (38). We retained *E. coli*
193 TOP10, containing both pMeth and the shuttle vector plasmid, as the donor strain and
194 *E. coli* HB101, carrying pRK2013, as the helper strain (39). To support the growth of

195 the *E. coli* strains and *C. kluyveri* on the same plate, we tested the growth of the two
196 *E. coli* strains on RCM plates supplemented with varying ethanol concentrations (86-
197 342 mM, 0.5-2.0% [v/v]) under a N_2/CO_2 atmosphere. Both *E. coli* strains exhibited
198 normal growth up to 257 mM ethanol. We decided to use the highest ethanol
199 concentration because it is the closest to the ethanol level that we use to cultivate
200 *C. kluyveri* (342 mM), making it the optimum condition for co-cultivating these three
201 strains.
202 We evaluated different mating durations (24, 48, 72, 96, and 120 h) by selecting
203 potentially transformed cells on plates containing thiamphenicol and trimethoprim. After
204 24 h, individual colonies were visible (**Figure S2A**). However, when extending mating
205 times from 48 h to 120 h, individual colonies became indistinguishable on selective
206 plates, requiring re-streaking to isolate single colonies (**Figure S2B)**. In the next step,
207 we successfully verified the presence of the shuttle vector plasmid inside *C. kluyveri*
208 cells *via* colony PCR (**Figure 3A**), and we sequenced the 16S rRNA gene to verify pure
209 cultures (**Figure 3B**). From these findings, we conclude that longer mating times
210 between 48 and 120 h enhance or at least do not adversely affect the transformation
211 efficiency of the cells.
212

213 **Heterologous gene expression as proof of concept**

214 To expand the product portfolio of *C. kluyveri*, we aimed to enable the conversion of *n*-
215 butyrate and *n*-caproate into *n*-butanol and *n*-hexanol. This was achieved by
216 introducing the *adhE2* gene from *C. acetobutylicum* into the shuttle vector plasmid
217 pMTL83151 under the control of its native promoter, which is P_{adhE2}. *adhE2* encodes a
218 bifunctional alcohol dehydrogenase, which catalyzes both the conversion of acyl-CoA
219 to the corresponding aldehyde in the first step and the reduction of the aldehyde to the
220 respective alcohol in the second step (40). After successful transformation of the

221 plasmid into *C. kluyveri* cells, we observed the production of alcohols corresponding to
222 the chain length of the carboxylates produced. However, preliminary measurements of
223 the alcohols produced by *C. kluyveri* pPadhE2_adhE2 revealed relatively low alcohol
224 concentrations (*n*-butanol: 1.87 mM, *n*-hexanol: 3.15 mM). To increase alcohol
225 production, we tested two conditions: **1)** increasing the expression of the *adhE2* gene
226 by using a stronger promoter (41); and **2)** introducing an NADPH-dependent alcohol
227 dehydrogenase because NADPH represents a more powerful co-factor than NADH
228 (42) and the use of NADH by AdhE2 potentially lowers the NADH/NAD+ ratio too much.
229 Therefore, using NADPH as an alternative co-factor could be advantageous for *n*-
230 butanol and *n*-hexanol production
231 To address these limitations, we enhanced *adhE2* expression by replacing the native
232 promoter with the reportedly stronger P_{thl} promoter from *C. acetobutylicum* (43, 44),
233 which resulted in higher *n*-butanol and *n*-hexanol concentrations (*n*-butanol: 2.73 mM,
234 *n*-hexanol: 3.25 mM) compared to the P_{adhE2} promoter. To further increase alcohol
235 production, we introduced the *bdhB* gene from *C. acetobutylicum*, encoding butanol
236 dehydrogenase B. Unlike AdhE2, BdhB uses NADPH as a co-factor for converting
237 aldehydes to alcohols (45, 46). Since BdhB exclusively catalyzes the second step from
238 the aldehyde to the alcohol (47), we retained AdhE2 to ensure acyl-CoA conversion to
239 the corresponding aldehyde. Thus, we tested three constructs on the shuttle vector
240 plasmid pMTL83151: **1)** pPadhE2_adhE2; **2)** pPthl_adhE2; and **3)** pPthl_adhE2_bdhB
241 and used the pMTL83151 vector as the negative control in a growth experiment
242 (**Figure 4**). We successfully transformed *C. kluyveri* cells with the three constructs and
243 the negative control and evaluated the resulting phenotypes. Notably, during the
244 conjugation process, we observed that DNA transfer for the plasmid encoding both
245 *adhE2* and *bdhB* was only successful after 72 h of mating.
246

247 ***n*-Butanol and *n*-hexanol production of the different strains**

248 In bottle experiments, *C. kluyveri* pPadhE2_adhE2, *C. kluyveri* pPthl_adhE2_bdhB,
249 and the negative control exhibited comparable growth with doubling times between 4.5
250 and 6 h (**Figure 4A**). In comparison, the three replicates of *C. kluyveri* pPthl_adhE2
251 started to grow at different times after inoculation, thus, leading to higher standard
252 deviations, not only for the OD_{600} but also for substrate and product concentrations for
253 this strain. However, the growth rates were similar to the other strains tested (data not
254 shown). Unfortunately, several attempts to repeat the growth experiment failed due to
255 a high mutation rate in the promoter region of *adhE2* in *C. kluyveri* pPthl_adhE2.
256 Average *n*-butanol and *n*-hexanol production was first observed after 33 h for
257 *C. kluyveri* pPthl_adhE2_bdhB and after 38 h for *C. kluyveri* pPadhE2_adhE2
258 (**Figures 4B,C**). Due to the extended lag phase and high standard deviations (up to
259 54% for *n*-butanol and 173% for *n*-hexanol), *C. kluyveri* pPthl_adhE2 was the last strain
260 starting to produce *n*-butanol and *n*-hexanol (first production observed between 61 h
261 and 81 h, data not shown), resulting in a slower average alcohol production than the
262 other replicates.

263 Regarding *n*-butanol production, *C. kluyveri* pPthl_adhE2_bdhB reached a maximum
264 concentration of 4.2 ± 0.0 mM, whereas *C. kluyveri* pPadhE2_adhE2 and *C. kluyveri*
265 pPthl_adhE2 exhibited similar *n*-butanol production levels (**Figure 4B**). In line with this
266 observation, *C. kluyveri* pPthl_adhE2_bdhB also achieved the highest *n*-hexanol
267 concentration (3.7 ± 0.6 mM), followed by *C. kluyveri* pPthl_adhE2 (2.3 ± 0.4 mM).
268 *C. kluyveri* pPadhE2_adhE2 produced the lowest amount of *n*-hexanol (2.2 ± 0.4 mM)
269 (**Figure 4C**). The difference in *n*-hexanol production between *C. kluyveri* pPthl_adhE2
270 and *C. kluyveri* pPadhE2_adhE2 likely would have been notably higher if *C. kluyveri*
271 pPthl_adhE2 had exhibited more consistent growth across the replicates. Also, a
272 longer experiment duration might have further highlighted a potential disparity.

273 Interestingly, both strains carrying P_{thl} started producing the corresponding alcohols at
274 lower *n*-butyrate and *n*-caproate concentrations (28.6 ± 10.3 mM and 15.6 ± 12.1 mM,
275 and 34.2 ± 1.4 mM and 21.7 ± 2.3 mM, respectively) (**Figures 4B,C)**. In contrast,
276 *C. kluyveri* pPadhE2_adhE2 started *n*-butanol and *n*-hexanol production at
277 42.6 ± 2.6 mM *n*-butyrate and 38.7 ± 5.3 mM *n*-caproate (**Figures 4B,C** and
278 **Figures S3C,D)**. Remarkably, *C. kluyveri* pPthl_adhE2_bdhB converted most acyl-
279 CoA into the corresponding alcohol, formed more *n*-butyrate than the other strains, and
280 reached the highest OD_{600} (**Figures 4A** and **Figures S3C,D)**. It produced 30% less *n*-
281 caproate than the other alcohol-producing strains and approximately 35% less than
282 the negative control (**Figure S3D)**. Due to the lower *n*-caproate production, its
283 conversion rate for substrate carbon into product carbon (*n*-butyrate, *n*-caproate, *n*-
284 butanol, and *n*-hexanol) only reached 53%, whereas the other strains converted 62-
285 67% of it (**Figures 4B,C and Figure S3**). Further, *C. kluyveri* pPthl_adhE2_bdhB
286 showed a higher acetate-to-ethanol ratio at the end of the experiment (0.16) than the
287 other strains (0.10-0.12) (**Figures S3A,B)**.

288 **DISCUSSION**

289 Our results show that: **1)** adapting the growth conditions for *C. kluyveri* on solid
290 DSMZ52 medium; **2)** determining the MIC of thiamphenicol; and **3)** counteracting
291 restriction modification barriers enabled successful DNA transfer of a shuttle vector
292 plasmid into *C. kluyveri* cells *via* conjugation after 24 h of mating. However, extending
293 the mating time to 48 h improved the transformation efficiency. Notably, transferring
294 the plasmid pPthl_adhE2_bdhB (8.234 kbp) was only successful after 72 h, suggesting
295 that shuttle vectors with critical genes or an increased size may require extended
296 mating times. This extension has been shown to improve conjugation efficiencies
297 overall (48).

298 All generated strains, but the negative control, showed plasmid-based gene expression
299 of the *adhE2* and *bdhB* genes from *C. acetobutylicum*. This led to phenotypically
300 modified *C. kluyveri* strains that were capable of producing *n*-butanol and *n*-hexanol.
301 In line with our expectations, both replacing P_{adhE2} with the reportedly stronger P_{thl}
302 promoter and introducing a second, NADPH-dependent butanol dehydrogenase
303 resulted in enhanced *n*-butanol and *n*-hexanol production. The clear variability
304 observed in the lag phase duration among the replicates of *C. kluyveri* pPthl_adhE2
305 distorted the calculated mean values. This statistical distortion resulted in an artificial
306 lowering of the estimated growth rate because the extended lag phases of some
307 replicates disproportionately influenced the overall growth calculations. This bias not
308 only lowers the slope of the OD_{600} but also needs to be considered for the graphs
309 representing the substrates and products. A potential explanation for the extended lag
310 phase is cell stress caused by the P_{thl} promoter, which is stronger than P_{adhE2}. Because
311 AdhE2 catalyzes both reactions of acyl-CoA to aldehyde and aldehyde to alcohol, it
312 may have a higher affinity towards the first reaction in *C. kluyveri*. Hence, the promoter

313 exchange could lead to aldehyde accumulation, which is known to be toxic (49, 50),
314 causing cell stress and impaired cells.
315 The batch experiment provided compelling evidence supporting the hypothesis that
316 the combination of the P_{thl} promoter and solely the *adhE2* gene exhibits toxicity. This
317 toxicity was demonstrated conclusively by metabolic impairment: across three
318 independent growth experiments, none of the *C. kluyveri* pPthl_adhE2 replicates
319 produced detectable levels of either *n*-butanol or *n*-hexanol. In contrast, only one
320 experiment resulted in the successful production of the alcohols. Sequencing of the
321 non-alcohol-producing cultures revealed that all contained a deletion in the P_{thl} region
322 (**Figure S4A**), suggesting a selection pressure against the expression of *adhE2*.
323 Additionally, sequencing *C. kluyveri* pPthl_adhE2 cultures, which produced *n*-butanol
324 and *n*-hexanol, revealed a less defined baseline in the promoter region (**Figure S4B**),
325 indicating that a fraction of the cells had already mutated. Given these findings, we
326 cannot rule out that an unmutated pure culture of *C. kluyveri* pPthl_adhE2 could have
327 performed better. Nonetheless, while using a stronger promoter enhanced the
328 production of *n*-hexanol, adding the butanol dehydrogenase presumably helped
329 accelerate aldehyde removal. This prevented toxic accumulation and resulted in a
330 stable, mutation-free strain.
331 Furthermore, we observed reduced formation of *n*-caproate by *C. kluyveri*
332 pPthl_adhE2_bdhB despite reaching the highest OD_{600} of all strains. This might be due
333 to a more balanced use of the co-factors NADH and NADPH. Both co-factors are
334 utilized to prevent excessive depletion of NADH, which would result in a reduced
335 $NADH/NAD^+$ ratio. This results in a higher NADH reducing capability and increased
336 alcohol production (51). Additionally, improved recycling of the co-factors could explain
337 the lower final concentration of *n*-caproate. Since NADH and NADPH are used as
338 electron donors for alcohol production, they are less available for other processes,

such as the formation of carboxylates (28). As a result, these reactions occur less frequently, leading to a decrease in *n*-caproate production.

The genetic system demonstrated in this study enabled plasmid-based gene expression, leading to heterologous production of *n*-butanol and *n*-hexanol by *C. kluyveri*. Besides expanding the product portfolio of this microbe, our research represents the first step towards developing a broader toolkit for *C. kluyveri*, including genome editing techniques (*e.g.*, homologous recombination, CRISPR-based methods). Consequently, the genetic accessibility of the model microbe for chain elongation is a precondition for further research on the reverse ß-oxidation pathway, which holds strong industrial potential. Therefore, gaining a deeper understanding of this pathway, both on a genetic level and in terms of the enzymes involved in their central energy metabolism, is crucial to enhancing its productivity.

351 # MATERIALS AND METHODS

352 ## Microbial strains, media, and cultivation

353 *C. kluyveri* DSM555 was obtained from the DSMZ (Braunschweig, Germany) and used
354 as the wild-type strain. Unless stated otherwise, all *C. kluyveri* strains in this study were
355 cultivated in DSMZ52 medium for which 2.5 g/L $NaHCO_3$ was used to buffer the
356 medium instead of Na_2CO_3. Cultures were grown in 100-mL medium with a headspace
357 of 140 mL under an N_2/CO_2 (80/20) atmosphere. Both liquid cultures and plates
358 (containing 0.8% [v/v] Bacto agar) were incubated at 37°C until visible growth was
359 observed. When required, the medium was supplemented with 5 µg/mL thiamphenicol
360 and 10 µg/mL trimethoprim for selection. All genetic manipulations of *C. kluyveri* were
361 conducted under strict anoxic conditions.
362 Unless otherwise noted, *E. coli* HB101 pRK2013 and *E. coli* TOP10 strains were grown
363 in liquid Luria-Bertani (LB) medium or on LB plates containing 1.5% agar. For plasmid
364 selection and maintenance, the medium was supplemented with 100 µg/mL ampicillin
365 (for liquid cultures), 100 µg/mL carbenicillin (for plates), 30 µg/mL chloramphenicol, or
366 30 µg/mL kanamycin. IPTG was added at a concentration of 500 mM to induce the
367 expression of the methyltransferase encoded on pMeth.
368

369 ## Optimization of the plating efficiency

370 The variables (**Table S1**) were systematically adjusted one at a time to determine the
371 optimal plating conditions, while all other conditions remained identical. The resulting
372 outcomes were compared to the previously identified best conditions. Both the
373 modified condition and the previously best-performing combination of conditions were
374 tested using the same culture conditions and inoculation volume (4% [v/v]) with
375 simultaneous incubation. The inoculum was serially diluted by increasing the dilution

376 factor by a magnitude of 10, reaching a final dilution of 1:100,000, and each dilution
377 was plated in duplicates for both conditions. Colony counts were performed by
378 capturing images using the UVP GelStudio system (Analytic Jena, Jena, Germany)
379 and analyzed with the integrated colony-count software. The plating conditions yielding
380 the highest colony count were determined to be the updated optimal combination, and
381 the following variable was tested accordingly.
382

383 **Restriction digest**

384 10 mL of a late exponential phase *C. kluyveri* culture were harvested, washed twice
385 with phosphate-buffered saline (PBS) buffer (137 mM sodium chloride, 2.7 mM
386 potassium chloride, 10 mM sodium phosphate dibasic, and p1.8 mM potassium
387 phosphate monobasic), and resuspended in 300 µL PBS buffer. Cells were lysed using
388 bead-beating (30 sec, 6.5 m/s; FastPrep-24™, MP BioMedicals, Santa Ana, USA).
389 The lysing procedure was performed four times, and in between, the cells were kept
390 on ice for 3 min. The lysis was centrifuged at 2000 × *g* for 20 min at 4°C. To assess the
391 sensitivity of the respective plasmid to the native restriction enzymes of *C. kluyveri*,
392 5 µL of the supernatant were added to 13 µL plasmid (200 ng) and 2 µL rCutSmart™
393 buffer (New England Biolabs, Ipswich, Massachusetts, USA). The prepared reaction
394 mix was stored at 37°C for 1 to 24 h. Results were analyzed *via* gel electrophoresis
395 and potential corresponding restriction sites were analyzed *in silico* with SnapGene
396 (GSL Biotech LLC, San Diego, USA).
397

398 **PacBio sequencing**

399 High molecular weight DNA (25 ng/µL) was isolated with the NucleoSpin Microbial DNA
400 Mini kit for DNA (Macherey-Nagel, Düren, Germany) and sheared using 35 kb settings
401 with a Megaruptor 2 instrument (Diagenode, SA, Lüttich, Belgium). Average insert

402 sizes were approximately 10 kb. Sheared fragments were used to prepare libraries
403 with the HiFi SMRTbell Express Template Prep Kit 2.0 (Pacific Biosciences, Menlo
404 Park, California, USA). The libraries were size-selected with a BluePippin system
405 (SageScience, Beverly, USA) with 17 kb cutoff in a 0.75% DF Marker S1 High-Pass 6-
406 10 kb vs3 gel cassette (Biozym, Hamburg, Germany). The library was sequenced with
407 sequencing primer v2 (Pacific Biosciences, #101-847-900) and 4 h of pre-extension
408 time on a single SMRT Cell with the Sequel II system using Binding Kit 2.0.
409

410 **Methylation profiling**

411 Reads were demultiplexed using Lima (52) and converted into High-Fidelity (HiFi)
412 reads retaining kinetic information with Circular Consensus Sequencing (53). BAM files
413 were converted to FASTQ with bam2fastx (54). Reads shorter than 1000 bp and the
414 lowest 5% of reads based on quality scores were discarded using Filtlong (55).
415 Trycycler (56) was used to subsample reads and generate a consensus sequence from
416 12 assemblies independently generated with Flye (57), Miniasm (58), and Raven (59).
417 HiFi reads were then aligned with the consensus assembly using pbmm2 (60), and
418 ipdSummary (61) was used to detect and classify DNA base-modifications from the
419 kinetic signatures. MotifMaker (62) was used to identify statistically significant
420 methylated motifs, with a minimum score threshold of 60. Motifs were retained if they
421 were identified for 90% or more possible sites in the genome. The native
422 methyltransferase of *C. kluyveri,* responsible for methylating the critical CCGG sites,
423 was identified using the REBASE database (37).
424

425 **Plasmid construction**

426 Plasmids (**Table S2**) were constructed with *E. coli* TOP10 and the respective primers
427 (**Table S3)**. The pUC19 vector (63) served as the backbone for the methylation plasmid

428 pMeth. The gene encoding the critical methyltransferase (CKL_2671) from *C. kluyveri*
429 was PCR amplified (Q5 polymerase, New England Biolabs (NEB), Ipswich, MA, USA)
430 from genomic DNA (NucleoSpin, Microbial DNA, Macherey-Nagel) and inserted into
431 the multiple cloning site *via* Gibson Assembly (NEBuilder, NEB). The lambda t1
432 terminator was introduced downstream of the CKL_2671 gene *via* PCR, amplifying the
433 plasmid with overlapping primers and transferring the linear DNA inside *E. coli*. The
434 same method was applied to remove the nucleotide sequence between the promoter
435 and the start codon of CKL_2671 to utilize the promoter present in the backbone (P_{lac}).
436 In the final step, the origin of replication (ORI) was exchanged from the pSC101 ORI
437 to the p15a ORI (64) by Gibson Assembly (NEBuilder, NEB) to ensure a low copy
438 number and compatibility with the shuttle vector plasmids for *C. kluyveri*. For *n*-butanol
439 and *n*-hexanol production, pMTL83151 (35) served as the backbone for all shuttle
440 vector plasmids. The DNA fragments *adhE2*, *bdhB*, P_{adhE2}, and P_{thl} from
441 *C. acetobutylicum* were PCR amplified (Q5 polymerase, NEB) from genomic DNA, and
442 the respective fragments were inserted into the plasmids *via* Gibson Assembly
443 (NEBuilder, NEB).
444

445 **Triparental conjugational DNA transfer**

446 We inoculated LB medium supplemented with ampicillin, chloramphenicol, and IPTG
447 (to induce the expression of the methyltransferase) with the donor strain *E. coli* TOP10,
448 carrying the desired plasmid and incubated the culture overnight. When both the donor
449 strain and the helper strain *E. coli* HB101 pRK2013, which was grown in LB medium
450 supplemented with 30 µL kanamycin, reached an OD_{600} of 0.6-0.8, 1 mL of each
451 culture was harvested by centrifugation (17,900 × *g*, 3 min). The resulting pellets were
452 suspended and mixed in PBS buffer. We again centrifuged the *E. coli* mixture (17,900
453 × *g*, 3 min) and transferred the received cell pellet into the anoxic chamber.

454 Subsequently, 2 mL of mid-exponential *C. kluyveri* wild-type culture (OD_{600}: 0.4-0.7)
455 was harvested *via* centrifugation (9.800 × *g*, 4 min) and resuspended in 50 µL RCM
456 under an N_2 atmosphere. This cell suspension was used to resuspend the *E. coli* cell
457 pellet. The cell mixture was then spot-plated on RCM plates (1.5% [v/v] agar)
458 containing 500 mM IPTG and 257 mM ethanol (1.5% [v/v]). Plates were incubated at
459 37°C in an N_2/CO_2 (80/20) atmosphere for up to 120 h. After mating, cells from the
460 mating spots were transferred *via* striking onto DSMZ52 plates containing
461 thiamphenicol to select for the respective plasmid. After cells had grown on the first
462 selective plate, they were streaked onto a thiamphenicol and trimethoprim-containing
463 DSMZ52 plate to select against *E. coli* strains. The resulting colonies were then further
464 analyzed.
465

466 **Molecular methods for analysis of genetically modified *C. kluyveri***

467 Direct colony PCR was conducted on both colonies and liquid cultures to confirm the
468 presence of the respective plasmid in *C. kluyveri* cells. Individual colonies were picked
469 and resuspended in 25 µL of 10 mM NaOH to extract the DNA template. For PCR
470 performed on liquid cultures, 100 µL of culture was sampled. In both cases, the cells
471 were lysed at 98°C for 10 min using a ThermoMixerC (Eppendorf, Hamburg,
472 Germany). For the PCR reactions, 1 µL of the lysate was utilized in two separate 10 µL
473 PCR reactions (PhirePlant (ThermoScientific™, Waltham, USA)) – one using plasmid-
474 specific primers and the other using *C. kluyveri*-specific primers. The results of the
475 reactions were analyzed *via* gel electrophoresis. Additionally, a 30 µL PCR reaction
476 targeting the 16S rRNA gene was performed using 3 µL of the lysate as a template.
477 The resulting PCR product was purified using the QIAquick PCR Purification Kit
478 (QIAGEN, Venlo, Netherlands) and subsequently analyzed *via* Sanger sequencing
479 (GENEWIZ, Leipzig, Germany) to verify a pure culture of *C. kluyveri*.

Analysis of compound concentration

To determine the concentrations of carboxylates (*e.g.*, acetate, *n*-butyrate, *n*-caproate) and alcohols (*n*-butanol and *n*-hexanol), an Agilent 7890B gas chromatograph (Agilent Technologies, Inc., Santa Clara, CA, USA) that were equipped with a DB-Fatwax UI capillary column (30 m x 0.25 mm x 0.25 μm) and flame ionization detector (FID) was used. Hydrogen served as the carrier gas, and the temperature program consisted of an initial temperature of 40°C for 3 min, ramped at 12°C/min to 160°C, followed by a further ramp of 20°C/min to 230°C with a 5-min hold. Ethyllactate was used as an internal standard at a concentration of 2 mM for quantifying carboxylates. The sampling volume was 1 mL of culture that was centrifuged (17,900 *g*, 3 min), and from which we stored the supernatant at -20°C until further analysis. Before measuring, the samples were thawed and filtered through a 0.2 μm polyvinylidene difluoride (PVDF) sterilefilter. For the analysis, samples were diluted at ratios of 1:2 for *n*-butanol and *n*-hexanol and 1:50 for MCCs measurements.

For ethanol concentration measurements, undiluted samples were analyzed using the LC-20 high-performance liquid chromatography (HPLC) system (Shimadzu, Nishinokyo Kuwabara-cho, Japan). The system was equipped with an Aminex-HPX-87H column, and 5 mM sulfuric acid was utilized as the mobile phase at a flow rate of 0.6 mL/min (LC-20AD). The oven temperature was maintained at 65°C (CTO-20AC), and the samples were cooled at 15°C in the autosampler unit.

ACKNOWLEDGEMENTS

We want to express our sincere gratitude to Silke Dauser and Heike Budde for performing the library preparation and PacBio sequencing. Further, the authors want to thank José Antonio Velázquez Gómez for supporting the HPLC analysis. Funding sources were the Max Planck Institute to L.T.A. as a Max Planck Fellow, the Alexander von Humboldt Foundation through the Alexander von Humboldt Professorship (L.T.A.), the Novo Nordisk Foundation through the CO_2 Research Center (CORC) with grant number NNF21SA0072700 (L.T.A.), the Deutsche Forschungsgesellschaft (DFG, German Research Foundation) through the Leibniz Prize (L.T.A.), and the Deutsche Forschungsgemeinschaft under Germany's Excellence Strategy – EXC 2124 – 390838134 (L.T.A.).

L.T.A. initiated the work. C.S., S.T.B., and L.T.A. designed the experiments. C.S., S.T.B., J.W.M., and K.G. performed laboratory experiments and analyzed the data. L.T.A. and S.T.B. supervised the project. C.S., L.T.A., J.W.M., and S.T.B. wrote the manuscript, while all edited the paper and approved the final version.

We declare no conflict of interest.

REFERENCES

1. Masson-Delmotte V, Zhai P, Pirani A, Connors SL, Péan C, Berger S, Caud N, Chen Y, Goldfarb L, Gomis MI, Huang M, Leitzell K, Lonnoy E, Matthews JBR, Waterfield T, Yelekci O, R Y, Zhou B. 2022. Climate change 2021: the physical science basis, contribution of working group I to the sixth assessment report of the interfovernmetal panel on climate change. Cambridge University Press.
2. Angenent LT, Richter H, Buckel W, Spirito CM, Steinbusch KJ, Plugge CM, Strik DP, Grootscholten TI, Buisman CJ, Hamelers HV. 2016. Chain elongation with reactor microbiomes: open-culture biotechnology to produce biochemicals. Environmental Science & Technology 50:2796-2810.
3. Steinbusch KJ, Hamelers HV, Plugge CM, Buisman CJ. 2011. Biological formation of caproate and caprylate from acetate: fuel and chemical production from low grade biomass. Energy & Environmental Science 4:216-224.
4. Wang J, Yin Y. 2022. Biological production of medium-chain carboxylates through chain elongation: an overview. Biotechnology Advances 55:107882.
5. Marang L, Jiang Y, van Loosdrecht MC, Kleerebezem R. 2013. Butyrate as preferred substrate for polyhydroxybutyrate production. Bioresource Technology 142:232-239.
6. Szacherska K, Oleskowicz-Popiel P, Ciesielski S, Mozejko-Ciesielska J. 2021. Volatile fatty acids as carbon sources for polyhydroxyalkanoates production. Polymers 13:321.
7. de Araújo Cavalcante W, Leitão RC, Gehring TA, Angenent LT, Santaella ST. 2017. Anaerobic fermentation for *n*-caproic acid production: A review. Process Biochemistry 54:106-119.
8. Palkovits S, Palkovits R. 2019. The role of electrochemistry in future dynamic bio-refineries: a focus on (non-) kolbe electrolysis. Chemie Ingenieur Technik 91:699-706.
9. Harvey BG, Meylemans HA. 2014. 1-Hexene: a renewable C6 platform for full-performance jet and diesel fuels. Green Chemistry 16:770-776.
10. Gupta C, Prakash D, Gupta S. 2015. A biotechnological approach to microbial based perfumes and flavours. Journal of Microbiological Methods. doi.org/10.15406/jmen.20150100034.
11. Jeon BS, Moon C, Kim B-C, Kim H, Um Y, Sang B-I. 2013. *In situ* extractive fermentation for the production of hexanoic acid from galactitol by *Clostridium* sp. BS-1. Enzyme and Microbial Technology 53:143-151.
12. Serhan M, Mattar J, Debs L. 2016. Concentrated yogurt (labneh) made of a mixture of goats' and cows' milk: Physicochemical, microbiological and sensory analysis. Small Ruminant Research 138:46-52.
13. Van Immerseel F, De Buck J, Boyen F, Bohez L, Pasmans F, Volf J, Sevcik M, Rychlik I, Haesebrouck F, Ducatelle R. 2004. Medium-chain fatty acids decrease colonization and invasion through *hilA* suppression shortly after infection of chickens with *Salmonella Enterica* serovar Enteritidis. Applied and Environmental Microbiology 70:3582-3587.
14. Huang CB, Alimova Y, Myers TM, Ebersole JL. 2011. Short-and medium-chain fatty acids exhibit antimicrobial activity for oral microorganisms. Archives of Oral Biology 56:650-654.
15. Zhang J, Taylor S, Wang Y. 2016. Effects of end products on fermentation profiles in *Clostridium carboxidivorans* P7 for syngas fermentation. Bioresource Technology 218:1055-1063.

16. Liu P, Jarboe LR. 2012. Metabolic engineering of biocatalysts for carboxylic acids production. Computational and Structural Biotechnology Journal doi.org/10.5936/csbj.201210011
17. Roghair M, Hoogstad T, Strik DP, Plugge CM, Timmers PH, Weusthuis RA, Bruins ME, Buisman CJ. 2018. Controlling ethanol use in chain elongation by CO_2 loading rate. Environmental Science & Technology 52:1496-1505.
18. Gervajio GC. 2005. Fatty acids and derivatives from coconut oil. In Bailey's industrial oil and fat products. John Wiley & Sons, Inc: Hooboken, NJ, USA, 2005. ISBN 9780471678496 6:1-56.
19. Schmitz LM, Kreitli N, Obermaier L, Weber N, Rychlik M, Angenent LT. 2024. Power-to-vitamins: producing folate (vitamin B9) from renewable electric power and CO_2 with a microbial protein system. Trends in Biotechnology 42:1691-1714.
20. Fernández-Blanco C, Robles-Iglesias R, Naveira-Pazos C, Veiga MC, Kennes C. 2023. Production of biofuels from C1-gases with *Clostridium* and related bacteria—recent advances. Microbial Biotechnology 16:726-741.
21. Werner JJ, Knights D, Garcia ML, Scalfone NB, Smith S, Yarasheski K, Cummings TA, Beers AR, Knight R, Angenent LT. 2011. Bacterial community structures are unique and resilient in full-scale bioenergy systems. Proceedings of the National Academy of Sciences 108:4158-4163.
22. Agler MT, Spirito CM, Usack JG, Werner JJ, Angenent LT. 2012. Chain elongation with reactor microbiomes: upgrading dilute ethanol to medium-chain carboxylates. Energy & Environmental Science 5:8189-8192.
23. Richter H, Molitor B, Diender M, Sousa DZ, Angenent LT. 2016. A narrow pH range supports butanol, hexanol, and octanol production from syngas in a continuous co-culture of *Clostridium ljungdahlii* and *Clostridium kluyveri* with in-line product extraction. Frontiers in Microbiology 7:1773.
24. Diender M, Stams AJ, Sousa DZ. 2016. Production of medium-chain fatty acids and higher alcohols by a synthetic co-culture grown on carbon monoxide or syngas. Biotechnology for Biofuels 9:1-11.
25. Schneider M, Bäumler M, Lee NM, Weuster-Botz D, Ehrenreich A, Liebl W. 2021. Monitoring co-cultures of *Clostridium carboxidivorans* and *Clostridium kluyveri* by fluorescence *in situ* hybridization with specific 23S rRNA oligonucleotide probes. Systematic and Applied Microbiology 44:126271.
26. Bäumler M, Schneider M, Ehrenreich A, Liebl W, Weuster-Botz D. 2021. Synthetic co-culture of autotrophic *Clostridium carboxidivorans* and chain elongating *Clostridium kluyveri* monitored by flow cytometry. Microbial Biotechnology 15:1471-1485.
27. Gildemyn S, Molitor B, Usack JG, Nguyen M, Rabaey K, Angenent LT. 2017. Upgrading syngas fermentation effluent using *Clostridium kluyveri* in a continuous fermentation. Biotechnology for Biofuels 10:1-15.
28. Thauer RK, Jungermann K, Decker K. 1977. Energy conservation in chemotrophic anaerobic bacteria. Bacteriological Reviews 41:100-180.
29. Thauer R, Jungermann K, Henninger H, Wenning J, Decker K. 1968. The energy metabolism of *Clostridium kluyveri*. European Journal of Biochemistry 4:173-180.
30. Li F, Hinderberger J, Seedorf H, Zhang J, Buckel W, Thauer RK. 2008. Coupled ferredoxin and crotonyl coenzyme A (CoA) reduction with NADH catalyzed by the butyryl-CoA dehydrogenase/Etf complex from *Clostridium kluyveri*. Journal of Bacteriology 190:843-850.

31. Scherf U, Söhling B, Gottschalk G, Linder D, Buckel W. 1994. Succinate-ethanol fermentation in *Clostridium kluyveri*: purification and characterisation of 4-hydroxybutyryl-CoA dehydratase/vinylacetyl-CoA Δ3-Δ2-isomerase. Archives of Microbiology 161:239-245.
32. Molitor B, Kirchner K, Henrich AW, Schmitz S, Rosenbaum MA. 2016. Expanding the molecular toolkit for the homoacetogen *Clostridium ljungdahlii*. Scientific Reports 6:1-10.
33. Kuehne SA, Heap JT, Cooksley CM, Cartman ST, Minton NP. 2011. ClosTron-mediated engineering of *Clostridium*, p 389-407, Strain Engineering. Springer.
34. Klask C-M, Jäger B, Casini I, Angenent LT, Molitor B. 2022. Genetic evidence reveals the indispensable role of the *rseC* gene for autotrophy and the importance of a functional electron balance for nitrate reduction in *Clostridium ljungdahlii*. Frontiers in Microbiology 13:887578.
35. Heap JT, Pennington OJ, Cartman ST, Minton NP. 2009. A modular system for *Clostridium* shuttle plasmids. Journal of Microbiological Methods 78:79-85.
36. Schneider MI. 2024. Entwicklung von molekularbiologischen Werkzeugen für den sekundären Gärer *Clostridium kluyveri*. Technische Universität München.
37. Roberts RJ, Vincze T, Posfai J, Macelis D. 2015. REBASE—a database for DNA restriction and modification: enzymes, genes and genomes. Nucleic Acids Research 43:D298-D299.
38. Lesiak JM, Liebl W, Ehrenreich A. 2014. Development of an *in-vivo* methylation system for the solventogen *Clostridium saccharobutylicum* NCP 262 and analysis of two endonuclease mutants. Journal of Biotechnology 188:97-99.
39. Ditta G, Stanfield S, Corbin D, Helinski DR. 1980. Broad host range DNA cloning system for gram-negative bacteria: construction of a gene bank of *Rhizobium meliloti*. Proceedings of the National Academy of Sciences 77:7347-7351.
40. Fontaine L, Meynial-Salles I, Girbal L, Yang X, Croux C, Soucaille P. 2002. Molecular characterization and transcriptional analysis of *adhE2*, the gene encoding the NADH-dependent aldehyde/alcohol dehydrogenase responsible for butanol production in alcohologenic cultures of *Clostridium acetobutylicum* ATCC 824. Journal of Bacteriology 184:821-830.
41. Nevoigt E, Kohnke J, Fischer CR, Alper H, Stahl U, Stephanopoulos G. 2006. Engineering of promoter replacement cassettes for fine-tuning of gene expression in *Saccharomyces cerevisiae*. Applied and Environmental Microbiology 72:5266-5273.
42. Zhou Z, Jing Y, Wei S, Zhang Q, Peng S, An X, Li H. 2023. Enhancement of butanol production in *Clostridium acetobutylicum* SE25 through oxidation-reduction potential regulation and analysis of its metabolic mechanisms. Fuel 331:125708.
43. Huang H, Chai C, Li N, Rowe P, Minton NP, Yang S, Jiang W, Gu Y. 2016. CRISPR/Cas9-based efficient genome editing in *Clostridium ljungdahlii*, an autotrophic gas-fermenting bacterium. ACS Synthetic Biology 5:1355-1361.
44. Hoffmeister S, Gerdom M, Bengelsdorf FR, Linder S, Flüchter S, Öztürk H, Blümke W, May A, Fischer R-J, Bahl H. 2016. Acetone production with metabolically engineered strains of *Acetobacterium woodii*. Metabolic Engineering 36:37-47.
45. Yoo M, Bestel-Corre G, Croux C, Riviere A, Meynial-Salles I, Soucaille P. 2015. A quantitative system-scale characterization of the metabolism of *Clostridium acetobutylicum*. MBio 6:1-12.

46. Lee SY, Park JH, Jang SH, Nielsen LK, Kim J, Jung KS. 2008. Fermentative butanol production by Clostridia. Biotechnology and Bioengineering 101:209-228.
47. Foulquier C, Rivière A, Heulot M, Dos Reis S, Perdu C, Girbal L, Pinault M, Dusséaux S, Yoo M, Soucaille P. 2022. Molecular characterization of the missing electron pathways for butanol synthesis in *Clostridium acetobutylicum*. Nature Communications 13:4691.
48. Huisman JS, Benz F, Duxbury SJ, de Visser JAG, Hall AR, Fischer EA, Bonhoeffer S. 2022. Estimating plasmid conjugation rates: a new computational tool and a critical comparison of methods. Plasmid 121:102627.
49. Kunjapur AM, Prather KL. 2015. Microbial engineering for aldehyde synthesis. Applied and Environmental Microbiology 81:1892-1901.
50. Heldt D, Frank S, Seyedarabi A, Ladikis D, Parsons JB, Warren MJ, Pickersgill RW. 2009. Structure of a trimeric bacterial microcompartment shell protein, EtuB, associated with ethanol utilization in *Clostridium kluyveri*. Biochemical Journal 423:199-207.
51. Cheng C, Bao T, Yang S-T. 2019. Engineering *Clostridium* for improved solvent production: recent progress and perspective. Applied Microbiology and Biotechnology 103:5549-5566.
52. Armin Töpfer JM, Mitchell Robert Volger, Chan Ye, K L Weber. Lima - Demultiplex Barcoded PacBio Samples, v2.9.0. GitHub, https://github.com/PacificBiosciences/barcoding.
53. Töpfer A. CCS: Generate Highly Accurate Single-Molecule Consensus Reads (HiFi Reads), v6.4.0. GitHub, https://github.com/PacificBiosciences/ccs.
54. Armin Töpfer JM. PacBio BAM toolkit, v3.0.0. GitHub, https://github.com/pacificbiosciences/pbtk/.
55. Ryan Wick PM. Quality filtering tool for long reads, v0.2.1. GitHub, https://github.com/rrwick/Filtlong.
56. Wick RR, Judd LM, Cerdeira LT, Hawkey J, Méric G, Vezina B, Wyres KL, Holt KE. 2021. Trycycler: consensus long-read assemblies for bacterial genomes. Genome biology 22:1-17.
57. Kolmogorov M, Yuan J, Lin Y, Pevzner PA. 2019. Assembly of long, error-prone reads using repeat graphs. Nature Biotechnology 37:540-546.
58. Heng Li SM, Riku Walve, Ryan Wick. Ultrafast de novo assembly for long noisy reads (though having no censensus step), v0.3. GitHub, https://github.com/lh3/miniasm.
59. Robert Vaser IV, Andrew Zhang, Thanh Lee. De novo genome assembler for long uncorrected reads, v1.8.3. GitHub, https://github.com/lbcb-sci/raven.
60. Nat Echols DA, David Seifert, Lance Hepler, Derek W. Barnett, James Drake. Tools for detecting DNA modifications from single molecule, real-time sequencing data, v1.13.1. GitHub, https://github.com/PacificBiosciences/kineticsTools.
61. Patrick Marks NE, David Alexander, Mengjuei Hsieh, David Seifert, Lance Hepler, James Drake, Derek W. Barnett, Yuri D'Elia. Tools for detecting DNA modifications from single molecule, real-time sequencing data, v3.0.0. GitHub, https://github.com/PacificBiosciences/kineticsTools.
62. Maeder H. Find methylated motifs in prokaryotic genomes, v12. GitHub, https://github.com/wangdi2014/MotifMaker.
63. Yanisch-Perron C, Vieira J, Messing J. 1985. Improved M13 phage cloning vectors and host strains: nucleotide sequences of the M13mpl8 and pUC19 vectors. Gene 33:103-119.

718 64. Chang AC, Cohen SN. 1978. Construction and characterization of amplifiable
719 multicopy DNA cloning vehicles derived from the P15A cryptic miniplasmid.
720 Journal of Bacteriology 134:1141-1156.
721

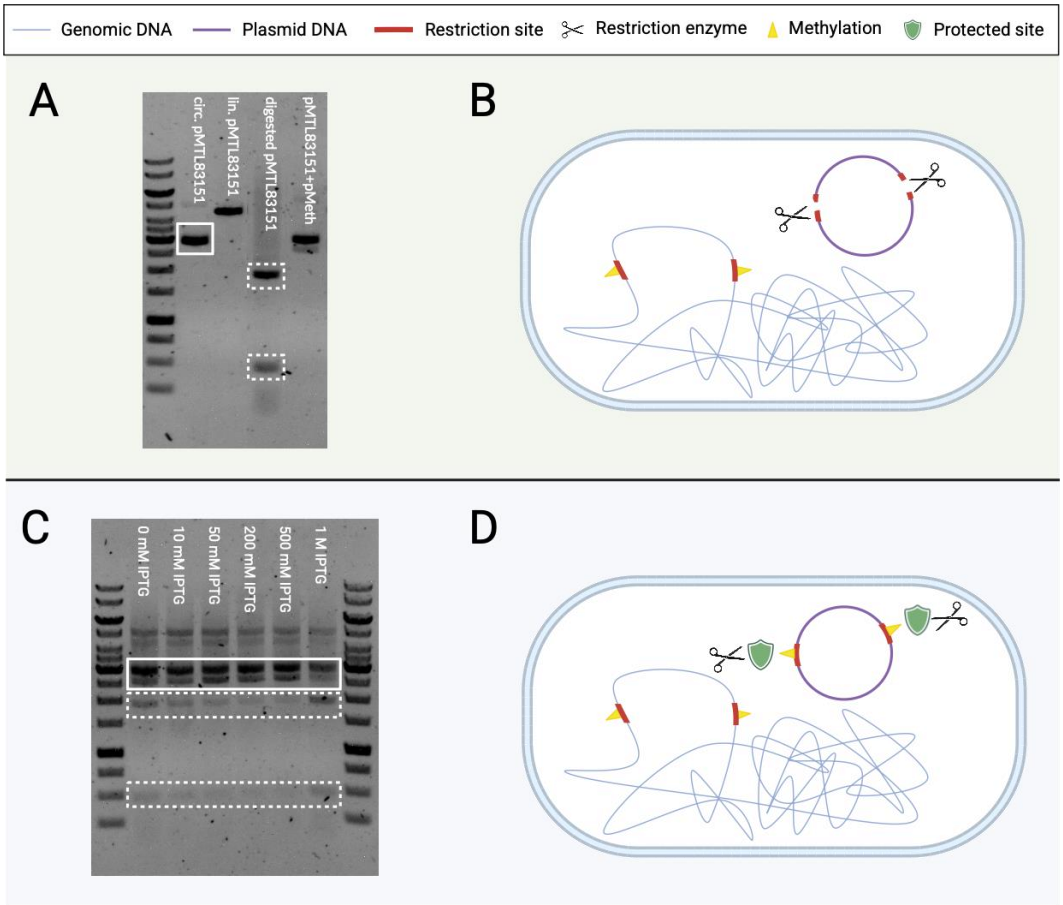

***Figure 1**. Restriction modification system of* C. kluyveri*. A) Restriction digest of the unmethylated pMTL83151 plasmid after 4 h. The solid-lined box in the 2nd lane shows the unrestricted, circular plasmid (~4.5 kbp), whereas the dashed-lined box in the 4th lane shows the vector digested by* C. kluyveri *cell lysate (fragment sizes: ~2 kbp, ~0.5 kbp). The linearized pMTL83151 vector in the 3rd lane (~4.5 kbp) and the mixture of circular plasmids pMTL83151 and pMeth (5th lane) serve as controls. B) In bacterial cells, DNA restriction serves as a defense mechanism against foreign DNA that either lacks methylation at the critical sites or shows a different methylation pattern from the native DNA of the respective bacterium. C) Restriction digest of* C. kluyveri*-specific methylated pMTL83151 after 24 h. Because the expression of the methyltransferase (CKL_2671) of* C. kluyveri *was controlled by the* P_{lac} *promoter, we tested different IPTG levels for*

induction (10°mM to 1 M). All induction levels result in minor restriction of pMTL83151 highlighted with dashed boxes (fragment sizes: *~2 kbp and ~0.5 kbp), however, the restriction was clearly reduced and minimized. Best results with the least restriction were obtained for the induction with 500 mM IPTG. D) As a result of the same methylation pattern as the native DNA, the foreign DNA is protected from restriction by the bacterial restriction modification system. Created with BioRender.com.*

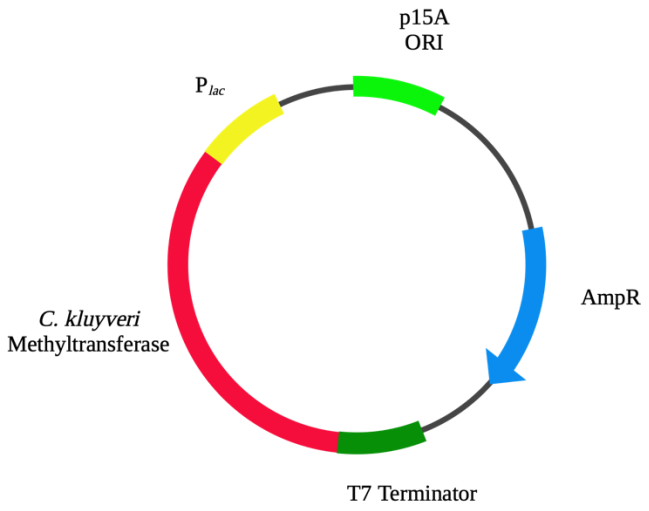

***Figure 2**. Plasmid map of pMeth based on pUC19. CKL_2671 was amplified from C. kluyveri genomic DNA and cloned into the multiple cloning site of pUC19. The T7 terminator was cloned into the plasmid and the ORI of puC19 was exchanged to the p15A ORI. Created with BioRender.com.*

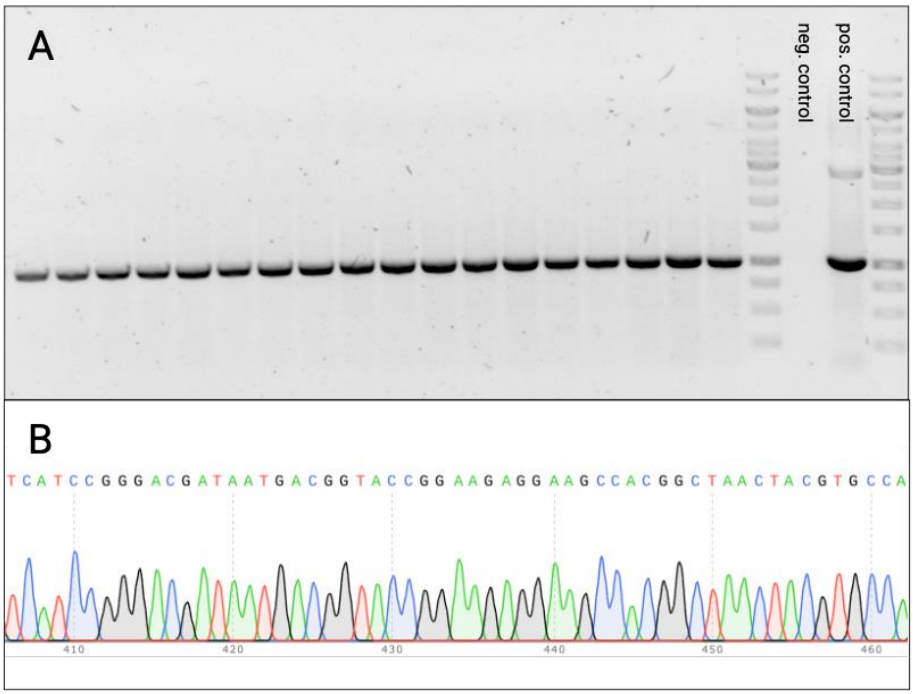

***Figure 3**. Verification of pMTL83151 inside* C. kluyveri *cells. A) We screened 18* C. kluyveri *colonies (lanes 1-18) for the presence of the plasmid pMTL83151 and verified its presence* via *colony PCR of the respective clones. Negative and positive (fragment size: ~1 kbp) controls are shown on the right side. The band corresponding to a longer fragment in the positive control results from the circular pMTL83151 plasmid, which served as template. B) Sanger Sequencing results of the 16S rRNA gene from the screened clones. All clones showed clear signals, confirming pure* C. kluyveri *pMTL83151 cultures. We show only one of the sequencing results here, which represents all tested clones. Created with BioRender.com.*

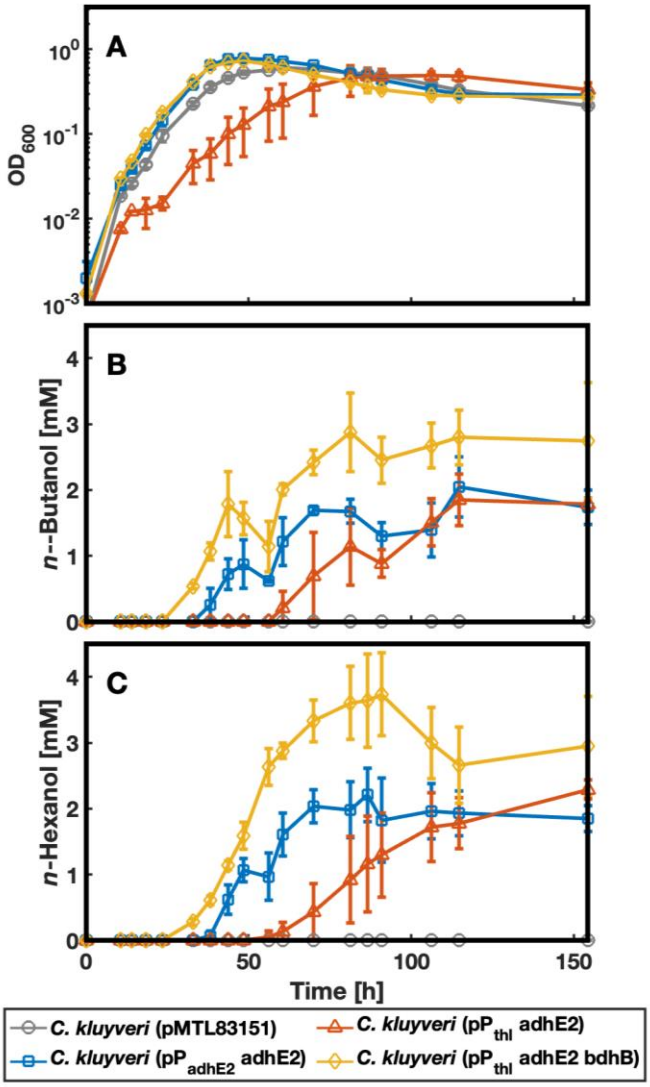

Figure 4. Results of the growth experiment. A) The growth behavior was measured by OD_{600}, showing that all strains but C. kluyveri *pPthl_adhE2 showed comparable growth. B)* C. kluyveri *pPthl_adhE2_bdhB reached the highest* n-*butanol concentration, whereas* C. kluyveri *pPadhE2_adhE2 and* C. kluyveri *pPthl_adhE2 showed comparable production levels. C) We observed the highest* n-*hexanol levels for* C kluyveri *pPthl_adhE2_bdhB, followed by* C. kluyveri *pPthl_adhE2. Created with MATLAB2024b.*